

# Manifestation of lattice distortions in the O 1s spectra in $\text{Ca}_{1-x}\text{Sr}_x\text{RuO}_3$

Ravi Shankar Singh and Kalobaran Maiti \*

*Department of Condensed Matter Physics and Materials Science,  
Tata Institute of Fundamental Research,  
Homi Bhabha Road, Colaba, Mumbai - 400 005, INDIA*

(Dated: February 4, 2008)

## Abstract

We investigate the effect of temperature on the electronic and crystal structures of  $\text{Ca}_{1-x}\text{Sr}_x\text{RuO}_3$  via the evolution of O 1s core level spectra as a function of temperature and composition,  $x$ . O 1s spectra in  $\text{SrRuO}_3$  exhibit a dominant sharp feature at all the temperatures with a small trace of impurity feature at higher binding energies. The spectra in Ca doped samples, however, exhibit two distinct features. Analysis of the experimental spectral functions and the band structure results suggest that different Madelung potential at the two types of oxygen sites in the orthorhombically distorted structure leads to such splitting in the O 1s spectra. Interestingly, the energy separation of these two features becomes smaller at low temperatures in the Ca dominated samples concomitant to the observation of non-Fermi liquid behavior in their bulk properties. Such temperature evolution, thus, indicates a direct connection of the lattice degrees of freedom with the electronic properties of these compounds.

Keywords: Strain induced level splitting, Strongly correlated systems, photoemission spectra

PACS numbers: 71.27.+a, 71.70.Fk, 79.60.Bm

---

\* Corresponding author: e-mail: kbmaiti@tifr.res.in      Fax: +91 22 2280 4610

## INTRODUCTION

Research in transition metal oxides has seen an explosive growth during last few decades due to discovery of many exotic properties such as high temperature superconductivity, giant magnetoresistance, insulator to metal transitions, quantum confinement effects *etc.* It is believed that all these novel material properties are essentially determined by the electronic states corresponding to the transition metal and oxygens forming the valence band (the highest occupied band). Numerous studies have been carried out to achieve microscopic understanding focussing primarily on the role of electron correlations in these material properties. The difficulty in such studies is that a large number of parameters such as electron correlation, electron-lattice interactions, charge carrier concentration, disorder *etc.* play crucial roles and it is virtually impossible to study the effect of a single parameter independently in a real system. In addition, significant mixing of the O  $2p$  and transition metal  $d$  states leads to further complexity of the problem.

Recently, there is a growing realization that the interaction of electrons and lattice vibrations is important to determine various exotic material properties such as colossal magnetoresistance [1], pseudogap phase in high-temperature superconductors [2], strange metallic behavior[3] *etc.* Since, oxygens in these materials have valency close to (2-) (electronic configuration,  $2s^22p^6$ ), the O  $2p$  levels are essentially filled. Thus, final state effects such as the correlation effects, core hole screening due to charge transfer from transition metals *etc.* will be negligible and the evolution of the O  $1s$  core levels are expected to efficiently manifest primarily the lattice effects.

In the present study, we investigate the role of electron-lattice interactions in the ground state properties of  $\text{Ca}_{1-x}\text{Sr}_x\text{RuO}_3$  via the evolution of O  $1s$  core levels as a function of temperature and composition.  $\text{SrRuO}_3$  is a perovskite compound and exhibits ferromagnetic long range order below  $\sim 160$  K [4, 5]. However, no magnetic long-range order is observed in isostructural,  $\text{CaRuO}_3$  down to the lowest temperature studied [4, 5, 6, 7]. Various investigations predict a non-Fermi liquid ground state in  $\text{CaRuO}_3$  in contrast to the Fermi-liquid behavior observed in  $\text{SrRuO}_3$  [6, 7]. Recently, it is shown that the correlation effects are significantly weak in both these compounds [8]. Band structure results using full potential augmented plane wave method suggest that Ca-O/Sr-O covalency plays the key role in determining the electronic as well as crystal structure in these systems, and the absence of long

range order in  $\text{CaRuO}_3$  has been attributed to the smaller Ru-O-Ru angle of  $150^\circ$  compared to  $165^\circ$  in  $\text{SrRuO}_3$  [9].

While all these studies throw some light on the electronic and magnetic properties of these systems, transition from Fermi liquid to non-Fermi liquid behavior is still a puzzle. A recent photoemission study using high-energy resolution reveals signature of particle-hole asymmetry and predict strong influence of phonons in the electronic excitation spectra in  $\text{CaRuO}_3$  in contrast to the case of  $\text{SrRuO}_3$ . It is now timely to investigate the lattice effects independently to achieve microscopic understanding of the electronic properties in these systems. We observe that multiple features appear in the oxygen  $1s$  spectra due to orthorhombic distortion of the crystal structure in  $\text{CaRuO}_3$ , while close to cubic structure of  $\text{SrRuO}_3$  leads to a single feature in the spectra. The photoemission results reveal significant temperature induced modification of the crystal lattice in Ca dominated compositions, while  $\text{SrRuO}_3$  appears to be very similar at all the temperatures studied.

## EXPERIMENTAL

High quality polycrystalline samples (large grain size achieved by long sintering at the preparation temperature) were prepared by solid state reaction method using ultra-high purity ingredients and characterized by  $x$ -ray diffraction (XRD) patterns and magnetic measurements as described elsewhere [4, 8]. Sharp XRD patterns reveal pure  $\text{GdFeO}_3$  structure at all the compositions studied with the lattice constants similar to those observed for single crystalline samples [5]. Photoemission measurements were carried out in an ultra-high vacuum chamber (base pressure lower than  $5 \times 10^{-11}$  torr) using SES2002 Scienta analyzer, and Al  $K\alpha$   $x$ -rays from monochromatic and twin sources. The energy resolutions were fixed at 0.3 eV and 0.9 eV for the measurements using monochromatic and twin sources, respectively. Sample surface was cleaned by *in situ* scraping. Reproducibility and cleanliness of the sample surface was confirmed after each trial of scraping.

## RESULTS AND DISCUSSIONS

In Fig. 1, we show the O  $1s$  core level spectra of  $\text{SrRuO}_3$  at different temperatures and photon sources. The Al  $K\alpha$  twin source spectrum at 300 K exhibit two distinct features.

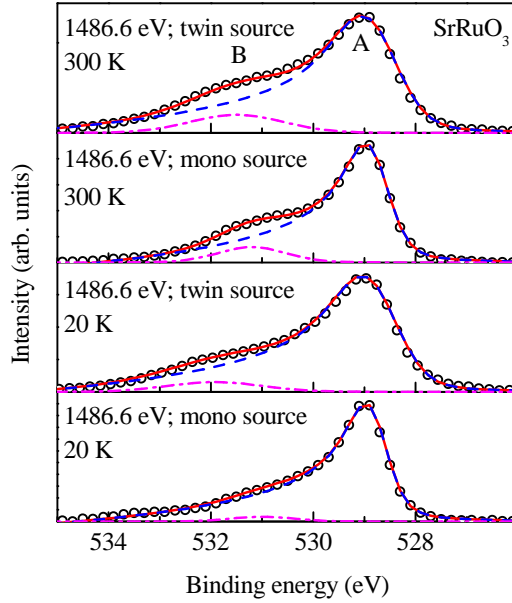


FIG. 1: O 1s core level spectra of SrRuO<sub>3</sub> at different temperatures.

The feature A appears at about 528.8 eV binding energy and has the largest intensity. The second feature B is significantly weak compared to A and appears around  $531.5 \pm 0.2$  eV. Since, O 2p levels are almost completely filled, the feature B cannot be attributed to photoemission signals due to different degrees of core hole screening in the photoemission final states as often observed in the core level spectra corresponding to transition metals and/or rare earths. Thus, this features is often used as a measure of the additional oxygens and/or foreign oxides adsorbed on the sample surface. Scraping the sample surface often leads to decrease in intensity of this feature confirming the above predictions. In the present case, the intensity of feature B could not be reduced further by repeated scrapings. In order to estimate the contribution of feature B in the total spectrum, we fit the experimental spectra by two Doniach-Šunjić lineshapes[10] as shown by dashed and dot-dashed lines in the figure. The simulated spectral function passing through the experimental data points represent a good fit. It is clear that the asymmetry of the feature B is significantly small compared to that for the feature A. The intensity of B is about 10% of the total intensity.

The second panel of Fig. 1 shows the O 1s signals from SrRuO<sub>3</sub> using monochromatic *x*-ray source, which has significantly improved energy resolution (0.3 eV). It is clear that the spectral features A and B are narrower and somewhat better defined. The relative intensity of the feature B is found to be about 9% of the total intensity similar to that observed in the case of twin source spectrum. The intensity of feature B reduces significantly with the

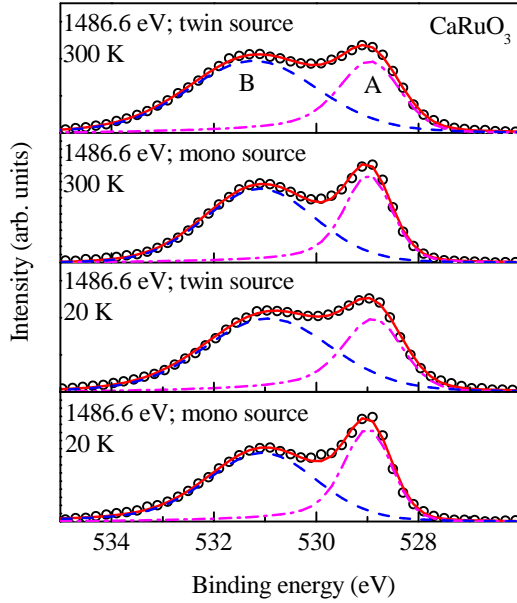


FIG. 2: O 1s core level spectra of CaRuO<sub>3</sub> at different temperatures.

decrease in temperature to 20 K (see third and fourth panel of Fig. 1) corresponding to un-monochromatized (6% of total intensity) and monochromatized source (< 3% of total intensity), respectively. It is to note here that the intensity of feature B is always found to be slightly higher in the twin source spectra compared to that in the monochromatic source spectra presumably due to spectral weight redistribution by the larger width of the incident light. These results establish that *it is possible to generate clean sample surface by scraping high quality polycrystalline samples.*

The O 1s spectra of CaRuO<sub>3</sub> are shown in Fig. 2. The two features A and B appear around 528.7 eV and 531.4 eV binding energies, respectively. Surprisingly, the feature B is always found to be significantly broad and intense with an integrated intensity higher than feature A. In order to investigate, if this large intensity appears due to the impurities at the sample surface, grain boundaries and/or due to multiple phases of CaRuO<sub>3</sub>, we have prepared 3 sets of samples. The sharp features in the *x*-ray diffraction patterns and absence of any additional peak suggest high quality and single phase of the samples. In addition, the magnetic measurements exhibit magnetic moment of 3  $\mu_B$ /fu in the paramagnetic phase of CaRuO<sub>3</sub> (2.7  $\mu_B$ /fu in SrRuO<sub>3</sub>), which is close to their spin-only value of 2.83  $\mu_B$  for  $t_{2g\uparrow}^3 t_{2g\downarrow}^1$  configurations at Ru sites [4, 5]. This suggests that the two peak structure in O 1s spectra might be intrinsic to this sample.

In order to investigate the origin of these two features, we have calculated the O 2s

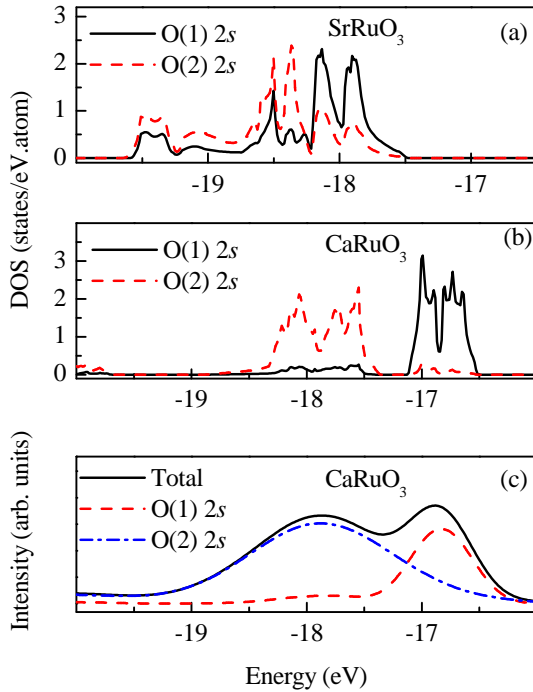


FIG. 3: The density of states of O  $2s$  core levels in (a)  $\text{SrRuO}_3$  and (b)  $\text{CaRuO}_3$  obtained by band structure calculations. The calculated results exhibit well separated O(1) and O(2) contributions in  $\text{CaRuO}_3$  compared to that in  $\text{SrRuO}_3$ . (c) The O  $2s$  density of states in  $\text{CaRuO}_3$  are broadened by a Gaussian to show the lineshape of the total spectral function.

core level density of states using state-of-the-art full potential linearized augmented plane wave (FP-LAPW) method (Wien2K software [11]). There are two types of oxygens present in the structure. If O(1) represent the apical oxygens of the  $\text{RuO}_6$  octahedra and O(2) represent those in the basal plane, there are one O(1) and two O(2) atoms in one formula unit. It is important to note here that the electron electron Coulomb interactions cannot be treated exactly in these calculations. Thus, binding energy of the core levels is often underestimated in the calculations compared to the experimental results. However, the effect due to Madelung potential can be captured reasonably well in these calculations. The details of the method of calculation is described elsewhere [9].

The calculated results for  $\text{SrRuO}_3$  and  $\text{CaRuO}_3$  are shown in Fig. 3(a) and 3(b), respectively. The O  $2s$  contributions in  $\text{SrRuO}_3$  appear very close to each other in Fig. 3(a). However, the density of states in  $\text{CaRuO}_3$  is significantly different. The separation between O(1)  $2s$  and O(2)  $2s$  contributions is more than 1 eV. If we broaden the two features with a Gaussian with a slightly different width, the lineshape of the resultant spectral function

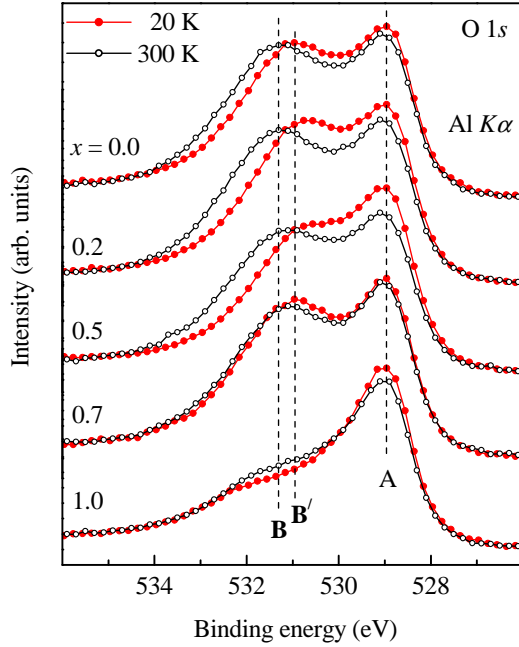


FIG. 4: O  $1s$  core level spectra of  $\text{Ca}_{1-x}\text{Sr}_x\text{RuO}_3$  for different values of  $x$  at 300 K and 20 K. All the spectra are collected using Al  $K\alpha$  un-monochromatized source.

shown in Fig. 3(c) is remarkably similar to that observed in Fig. 2. In order to investigate the intensity ratio of the two features in the experimental spectra, we fit the experimental spectra in Fig. 2 by a set to two Doniach-Šunjić lineshapes as done in the case of  $\text{SrRuO}_3$ . Interestingly, the intensity of the feature B is found to be about  $1.8 \pm 0.2$  times of the intensity of the feature A. These results, thus, reveal that the two peak structure in the O  $1s$  spectra in Fig. 2 is intrinsic and can be attributed to different Madelung potential at different oxygen sites.

Decrease in temperature leads to a shift in the peak position of feature B by about 0.2 eV towards lower binding energies. The relative intensity of the features remain almost similar at low temperatures. Notably, the charge transfer satellite in Ca  $2p$  core level spectra in  $\text{CaRuO}_3$  also moves towards lower binding energies with the decrease in temperature [12]. However, Sr  $3d$  core level spectra does not exhibit such effect in  $\text{SrRuO}_3$ . This clearly indicates that the decrease in temperature leads to a significant modification in the local structure involving Ca and O sites in  $\text{CaRuO}_3$ .

In order to investigate this effect across the whole composition range, we plot the O  $1s$  spectra in  $\text{Ca}_{1-x}\text{Sr}_x\text{RuO}_3$  for different values of  $x$  in Fig. 4. All the spectra are normalized by total integrated area under the curve. Two effects are clearly visible in the figure. Firstly,

the feature B is significantly strong even in the 70% Sr substituted sample. Thus, a small amount of Ca in the crystal lattice appears to introduce a significant structural distortion leading to two intense features as observed in  $\text{CaRuO}_3$ . Secondly, the feature B at 300 K shifts by about 0.2 eV to B' in the 20 K spectra for all  $x$  values upto  $x = 0.5$ . This shift becomes very small for  $x = 0.7$  and almost not significant for  $x = 1.0$ . This suggests that the temperature induced local distortion primarily appears in the Ca dominated compositions. Interestingly, the non-Fermi liquid behavior is also observed in the samples with similar compositions [6]. This study thus, provides an evidence of a direct relationship of the non-Fermi liquid behavior with the structural changes.

In summary, we investigate the evolution of O 1s core level spectra as a function of temperature and composition in  $\text{Ca}_{1-x}\text{Sr}_x\text{RuO}_3$  for various values of  $x$ . The spectra in  $\text{SrRuO}_3$  shows that high quality polycrystalline samples can be cleaned efficiently by *in situ* scraping. The scraped surface at low temperature appears to be almost free of any impurity. This is significant considering the fact that many systems exhibiting novel electronic properties can be studied efficiently using samples in polycrystalline forms, particularly where it is difficult to prepare single crystals.

The O 1s spectra in Ca substituted compositions exhibit two peak structure, which can be attributed to the difference in Madelung potential at different oxygen sites in the structure. Decrease in temperature leads to a significant modification in the local structure in the Ca dominated compositions. While this provides one possible explanation of the proximity of these compounds to the quantum criticality, it is highly desirable to investigate the issue further. We hope that these results would help to initiate further studies (*x*-ray diffraction, extended *x*-ray fine structure *etc.*) in this direction.

- 
- [1] A.J. Millis, Nature 392 (1998) 147.
  - [2] N. Mannella *et al.*, Nature 438 (2005) 474.
  - [3] K. Maiti, R.S. Singh, V.R.R. Medicherla, (unpublished); cond-mat/0604648.
  - [4] R.S. Singh, P.L. Paulose, K. Maiti, Solid State Physics (India), 49 (2004) 876.
  - [5] G. Cao, S. McCall, M. Shepard, J.E. Crow, R.P. Guertin, Phys. Rev. B 56 (1997) 321.
  - [6] P. Khalifah, I. Ohkubo, H. Christen, D. Mandrus, Phys. Rev. B 70 (2004) 134426; Y. S. Lee,



- Jaejun Yu, J. S. Lee, T. W. Noh, T.-H. Gimm, Han-Yong Choi, C. B. Eom, Phys. Rev. B 66 (2002) 041104(R).
- [7] L. Klein, L. Antognazza, T.H. Geballe, M.R. Beasley, A. Kapitulnik, Phys. Rev. B 60 (1999) 1448.
- [8] K. Maiti, R.S. Singh, Phys. Rev. B 71 (2005) 161102(R).
- [9] K. Maiti, Phys. Rev. B 73 (2006) 235110; cond-mat/0605553.
- [10] S. Doniach, M. Šunjić, J. Phys. C: Solid State Phys. 3 (1970) 285.
- [11] P. Blaha, K. Schwarz, G.K.H. Madsen, D. Kvasnicka, J. Luitz, **WIEN2k**, An Augmented Plane Wave + Local Orbitals Program for Calculating Crystal Properties, Karlheinz Schwarz, Techn. Universität Wien, Austria, 2001, (ISBN 3-9501031-1-2).
- [12] R.S. Singh, K. Maiti, (unpublished) (2006); cond-mat/0605552.